CAMPANELLI, A. R., CANDELORO DE SANCTIS, S., CHIESSI, E., D'ALAGNI, M., GIGLIO, E. & SCARAMUZZA, L. (1989). *J. Phys. Chem.* **93**, 1536–1542.
CANDELORO DE SANCTIS, S. & GIGLIO, E. (1979). *Acta Cryst.* B**35**, 2650–2655.
CANDELORO DE SANCTIS, S., CHIESSI, E. & GIGLIO, E. (1985). *J. Incl. Phenom.* **3**, 55–64.
CANDELORO DE SANCTIS, S., COIRO, V. M., GIGLIO, E., PAGLIUCA, S., PAVEL, N. V. & QUAGLIATA, C. (1978). *Acta Cryst.* B**34**, 1928–1933.
CANDELORO DE SANCTIS, S., GIGLIO, E., PAVEL, V. & QUAGLIATA, C. (1972). *Acta Cryst.* B**28**, 3656–3661.
CANDELORO DE SANCTIS, S., GIGLIO, E., PETRI, F. & QUAGLIATA, C. (1979). *Acta Cryst.* B**35**, 226–228.
COIRO, V. M., D'ANDREA, A. & GIGLIO, E. (1979). *Acta Cryst.* B**35**, 2941–2944.
COIRO, V. M., GIGLIO, E., MAZZA, F. & PAVEL, N. V. (1984). *J. Incl. Phenom.* **1**, 329–337.
CRAVEN, B. M. & DE TITTA, G. T. (1972). *J. Chem. Soc. Chem. Commun.* pp. 530–531.
CROMER, D. T. & MANN, J. B. (1968). *Acta Cryst.* A**24**, 321–324.
D'ALAGNI, M., DELFINI, M., GALANTINI, L. & GIGLIO, E. (1992). *J. Phys. Chem.* **96**, 10520–10528.
GAVUZZO, E., PAGLIUCA, S., PAVEL, N. V. & QUAGLIATA, C. (1972). *Acta Cryst.* B**28**, 1968–1969.
GIACOMELLO, G. & KRATKY, O. (1936). *Z. Kristallogr. A*, **95**, 459–464.
GIGLIO, E. (1984). *Inclusion Compounds*, Vol. 2, edited by J. L. ATWOOD, J. E. D. DAVIES & D. D. MCNICOL, ch. 7, pp. 207–229. London: Academic Press.
HIGUCHI, W. I. (1984). *Hepatology*, **4**, 161S–165S.
HOLZBACH, R. T. (1984). *Hepatology*, **4**, 173S–176S.
HOSTROW, J. D. (1984). *Hepatology*, **4**, 215S–222S.
JONES, E. L. & NASSIMBENI, L. R. (1990). *Acta Cryst.* B**46**, 399–405.
JONES, J. G., SCHWARZBAUM, S., LESSINGER, L. & LOW, B. W. (1982). *Acta Cryst.* B**38**, 1207–1215.
LESSINGER, L. (1982). *Cryst. Struct. Commun.* **11**, 1787–1792.
MAKIN, E. C. (1975). *New Developments in Separation Methods*, edited by E. GRUSHKA, pp. 49–64. New York/Basel: Marcel Dekker.
MIKI, K., KASAI, N., TSUTSUMI, H., MIYATA, M. & TAKEMOTO, K. (1987). *J. Chem. Soc. Chem. Commun.* pp. 545–546.
MIYATA, M. & TAKEMOTO, K. (1975). *Polymer Lett.* **13**, 221–223.
MIYATA, M., SHIBAKAMI, M., CHIRACHANCHAI, S., TAKEMOTO, K., KASAI, N. & MIKI, K. (1990). *Nature (London)*, **343**, 446–447.
PADMANABHAN, K., VENKATESAN, K. & RAMAMURTHY, V. (1984). *Can. J. Chem.* **62**, 2025–2028.
PADMANABHAN, K., VENKATESAN, K. & RAMAMURTHY, V. (1987). *J. Incl. Phenom.* **5**, 315–323.
PAVEL, N. V., QUAGLIATA, C. & SCARCELLI, N. (1976). *Z. Kristallogr.* **144**, 64–75.
PIACENTE, V., POMPILI, T., SCARDALA, P. & FERRO, D. (1991). *J. Chem. Thermodynam.* **23**, 379–396.
POPOVITZ-BIRO, R., TANG, C. P., CHANG, H. C., LAHAV, M. & LEISEROWITZ, L. (1985). *J. Am. Chem. Soc.* **107**, 4043–4058.
REISINGER, M. & LIGHTNER, D. A. (1985). *J. Inclusion Phenom.* **3**, 479–485.
SHELDRICK, G. M. (1976). *SHELX76. Program for Crystal Structure Determination.* Univ. of Cambridge, England.
TANG, C. P., POPOVITZ-BIRO, R., LAHAV, M. & LEISEROWITZ, L. (1979). *Isr. J. Chem.* **18**, 385–389.
WEISINGER-LEWIN, Y., VAIDA, M., POPOVITZ-BIRO, R., CHANG, H. C., MANNIG, F., FROLOW, F., LAHAV, M. & LEISEROWITZ, L. (1987). *Tetrahedron*, **43**, 1449–1475.
WIELAND, H. & SORGE, H. (1916). *Z. Physiol. Chem.* **97**, 1–27.

Acta Cryst. (1995). B**51**, 89–98

Structure of Ureido-Balhimycin

BY GEORGE M. SHELDRICK

Institut für Anorganische Chemie der Universität Göttingen, Tammannstrasse 4, *D*-37077 *Göttingen, Germany*

ERICH PAULUS* AND LÁSZLÓ VÉRTESY

Hoechst AG, D-65926 *Frankfurt am Main, Germany*

AND FRIEDEMANN HAHN

Stoe & Cie GmbH, Hilpertstrasse 10, *D*-64295 *Darmstadt, Germany*

(*Received* 17 *March* 1994; *accepted* 6 *September* 1994)

Abstract

The structure of the ureido derivative of balhimycin has been solved by Patterson vector superposition followed by iterative partial structure expansion, and refined against F^2 to R_1 = 0.0536 for 8949 $F > 4\sigma(F)$ and 0.0802 for all 11 977 image plate data. Crystal data: $C_{67}H_{74}Cl_2N_{10}O_{25}.27.75(H_2O)$, M_r = 1990.20, triclinic, $P1$, a = 17.909 (10), b = 18.466 (10), c = 18.873 (13) Å, α = 96.65 (5), β = 114.15 (5), γ = 114.78 (4)°, V = 4850 (5) Å^3, Z = 2, D_x = 1.363 Mg m^{-3}, Mo $K\alpha$, λ = 0.71073 Å, μ = 0.17 mm^{-1}, $F(000)$ = 2115, T = 293 K. This appears to be the first reported crystal structure of a naturally occuring member of the vancomycin family which has not been subject to degradation and ring rearrangement, and it appears likely that the conformation observed is close to that required for complex formation with cell-wall protein. It possesses a 'binding pocket' for the C-terminal carboxyl of this protein, which is consistent with suggestions based on NMR data. The two antibiotic molecules in the unit cell are bound by antiparallel hydrogen bonds to form a tight dimer, which may well persist in biological systems.

* Author to whom correspondence should be addressed.

The ureido-vancosamine is linked to a benzylic hydroxy group near the C-terminus rather than the glucose, as in vancomycin, and the Cl atoms lie on opposite sides of the molecule, as in vancomycin but not in its degradation product CDP-1. The structure of this ureido derivative implies that 4-oxo-vancosamine is present in balhimycin itself; this moiety could well be the 'missing link' in the biosynthesis of the epimeric sugars of vancosamine.

Introduction

Ureido-balhimycin is a natural glycopeptide antibiotic. It inhibits the growth of bacterial cell walls and is obtained as a minor product in the extraction of balhimycin, and may also be synthesized from balhimycin itself. Diseases caused by β-lactam resistant gram-positive bacteria are increasing dramatically (Boyce, 1989), so glycopeptide antibiotics that are able to overcome this resistance are becoming more important in chemotherapy (Nagarajan, 1991). The new antibiotic balhimycin (Nadkarni, Chatterjee, Patel, Desikan, Vijayakumar, Ganguli, Blumbach, Fehlhaber & Kogler, 1990), isolated from the culture fluid of *Amycolatopsis spec. DSM* 5908, is structurally related to vancomycin. The general structure of vancomycin was established by X-ray diffraction of the degradation product CDP-1 (Sheldrick, Jones, Kennard, Williams & Smith, 1978). However, subsequent NMR studies showed that one of the chlorophenyl rings rotates so that the two Cl atoms are on the same side of the molecule in CDP-1 but on opposite sides in the natural vancomycin, and that asparagine is replaced by isoaspartic acid during the degradation (Harris, Kopecka & Harris, 1983; Nagarajan, Merkel, Michel, Higgins, Hoehn, Hunt, Jones, Occolowitz, Schabel & Swartzendruber, 1988).

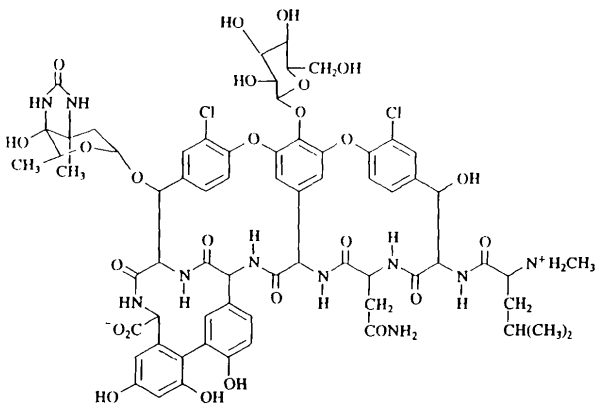

Removing the sugar residues in vancomycin and balhimycin results in the same compound. Despite this clue, it was not possible to deduce the structure of balhimycin unambiguously by spectroscopic methods, in part because the spectroscopic results were solvent dependent (Fehlhaber, Kogler & Vértesy, 1991). The main differences between the two compounds are that in vancomycin the vancosamine is attached to the glucose, whereas in balhimycin it is linked to a benzylic hydroxy group near the C-terminus, and in balhimycin the vancosamine hydroxy group is oxidized to a ketone. Good quality crystals were obtained from the reaction product of balhimycin with KNCO or urea. This product is identical to a minor component in the extraction of natural balhimycin, but the nature of this reaction (Stark, 1965) was also unclear before this crystal structure determination.

Since the crystals were found to have the space group $P1$, usually regarded as unfavourable for direct methods, with two molecules (263 unique non-H atoms including solvent) in the asymmetric unit, this structure also provided a severe test of methods solving the crystallographic phase problem.

Experimental

Preparation and crystal growth

Balhimycin (3 g, 2 mM) was dissolved in water (300 ml) at pH 6, KNCO (210 mg, 2.3 mM) was added and the reaction mixture stirred for 1 h. To remove the salt, the solution was treated with 150 ml of resin MCI Gel CHP 20 P (Mitsubishi Kasei Corporation, Tokyo). A gradient procedure with 30% isopropanol in 0.1% aqueous acetic acid was used to elute the reaction product, which was then freeze-dried. To obtain suitable crystals for the structure analysis, the compound was dissolved in water and the pH adjusted to 3.6 by adding trifluoroacetic acid. After 2 days, the initial crystals formed were removed, and after 6 weeks at room temperature a new crop of large transparent crystals had grown. These crystals proved to be very sensitive to any kind of mechanical treatment and disintegrated immediately on removal from aqueous solution. A crystal of dimensions 0.45 × 0.35 × 0.25 mm was sealed in a Lindemann glass capillary, together with a small amount of mother liquor.

Data collection

A laser-stimulated fluorescence image plate (Miyahara & Kato, 1984; Takahashi, Miyahara & Shibahara, 1985) was used as a two-dimensional area detector. During each exposure of 5 min, the diffraction pattern was stored as a latent image on the image plate. The plate was then scanned by a focused He–Ne laser beam of 150 μm diameter, which caused blue fluorescence light to be emitted with an intensity proportional to the number of absorbed X-ray photons. A photomultiplier tube and 16-bit ADC were used to record the emitted intensity, and a peak-minus-background algorithm was employed to obtain integrated reflection intensities. 190 frames were recorded at intervals of 1° about the rotation axis. The inner image plate radius

was 10 mm, the outer radius 90 mm, and the crystal to detector distance 70 mm. A total of *ca* 30 h was required for the data collection. A Stoe rotating anode with a Schneider generator was employed as the source of graphite-monochromated Mo $K\alpha$ radiation (λ = 0.71073 Å, 49 kV, 127 mA). 36 012 reflections were measured to a maximum 2θ of 51.8°, of which 17 239 were unique after merging reflections with identical indices and Friedel opposites; this corresponds to 91.5% completion at this limit. A crystal decay correction was applied during data reduction; between the first and last frame, the intensities decreased by 3.4%. This data set was employed for structure solution attempts. Subsequent analysis showed that the R_{int} value and also the R-indices for the least-squares refinement rose very rapidly for data with $2\theta > 45°$, indicating that these reflections were too weak to measure accurately, so data above this limit were not used for the structure refinement. We also confirmed that truncating the data to 2θ = 45° would not have had a significant influence on the structure solution. With hindsight it would have been better to collect the data with a somewhat larger plate-to-crystal distance. In addition, ten reflections, all with measured intensities close to zero, were removed because of suspected problems with the reflection indexing. The resulting 25 115 data were merged, averaging Friedel opposites and reflections with identical indices, to give 11 977 unique reflections that were used for the structure refinement. The lattice parameters determined by the image plate system were: a = 17.867 (18), b = 18.434 (20), c = 18.731 (20) Å, α = 97.06 (5), β = 113.71 (5), γ = 114.68 (5)°. Slightly different values were also obtained on a Siemens R3 computer-controlled four-circle diffractometer: a = 17.909 (10), b = 18.466 (10), c = 18.873 (13) Å, α = 96.65 (5), β = 114.15 (5), γ = 114.78 (4)°. Since diffractometer measurements would be expected to give a more accurate cell, the latter were employed throughout the structure analysis. Crystal data are presented in Table 1.*

Table 1. *Crystal data, data collection and refinement parameters*

Identification code	Balhi
Empirical formula	$[C_{67}H_{74}Cl_2N_{10}O_{25}]27.75H_2O$
Formula weight	1990.2
Temperature (K)	293 (2)
Wavelength (Å)	0.71073
Crystal system	Triclinic
Space group	$P\bar{1}$
Unit-cell dimensions	
a (Å)	17.909 (10)
b (Å)	18.466 (10)
c (Å)	18.873 (13)
α (°)	96.65 (5)
β (°)	114.15 (5)
γ (°)	114.78 (4)
Volume (Å^3)	4850 (5)
Z	2
D_x (Mg m^{-3})	1.363
Absorption coefficient (mm^{-1})	0.170
$F(000)$	2115
Crystal size (mm)	0.45 × 0.35 × 0.25
θ range for data collection (°)	4.4–22.5
Index ranges	
h	0→21
k	−22→20
l	−22→19
No. of measured reflections	25 115
No. of independent reflections	11 977
R_{int}	0.05
Absorption correction	None
Refinement method	Full-matrix-block least squares on F^2
Data; restraints; parameters	11 977; 1512; 2603
Goodness-of-fit on F^2	1.041
Final R [$I > 2\sigma(I)$]	R_1 = 0.0536, wR_2 = 0.1263
R (all data)	R_1 = 0.0802, wR_2 = 0.1423
Largest diff. peak and hole (e Å^{-3})	0.242 and −0.202

Solution of the phase problem

As anticipated, this structure proved to be too large for the direct methods available to us at the time, so we attempted to locate the four Cl atoms by automated Patterson superposition. Very recently we have, however, developed a 'direct method' which is able to solve this structure convincingly using the same data. The Patterson vector superposition method is discussed in detail in Buerger's (1959) book, where it is referred to as the 'vector shift' method; it has received only sporadic attention in recent years. In the absence of overlap in the Patterson function, a superposition minimum function based on a single correct heavy atom to heavy atom vector should consist of two images of the structure, related to one another by an inversion centre at the midpoint of the superposition vector. Two peaks, separated from each other by the superposition vector, should correspond to correct heavy atoms in both images of the structure, and there should be two further pairs of peaks corresponding to the other two Cl atoms in each of the two images. If a correct superposition vector can be found, the problem reduces to one of deciding which six peaks correspond to Cl atoms, and resolving them into two sets of four with two peaks in common. From chemical considerations it was known that none of the Cl—Cl distances should be shorter than *ca* 5 Å, and that there would be one Cl—Cl vector in the region of 8 Å in each of the two independent molecules.

A sharpened Patterson was calculated with coefficients $(E^3F)^{1/2}$ and the 20 highest peaks that were at least 5 Å from the nearest lattice point were used to construct superposition minimum functions using the same sharp-

* Lists of structure factors, anisotropic displacement parameters, H-atom coordinates and complete geometry have been deposited with the IUCr (Reference: HU0422). Copies may be obtained through The Managing Editor, International Union of Crystallography, 5 Abbey Square, Chester CH1 2HU, England.

Table 2. *Patterson interpretation*

x	*y*	*z*	Minimum distances / Patterson function value							
0.296	0.454	0.214	*A,B*							
0.704	0.546	0.786	12.78	*A,B*						
			41.8							
0.584	0.289	0.336	6.82	8.15	*A*					
			35.5	38.3						
0.416	0.711	0.664	8.15	6.82	11.51	*B*				
			38.3	35.5	0.0					
0.576	0.234	0.361	7.59	8.12	1.14	11.91	*B*			
			40.5	32.2	3.5	23.9				
0.424	0.766	0.639	8.12	7.59	11.91	1.14	10.60	*A*		
			32.2	40.5	23.9	3.5	26.0			
0.178	0.397	0.362	4.12	14.61	8.49	6.01	8.83	6.40	?	
			32.4	21.5	0.0	6.5	9.4	0.0		
0.822	0.603	0.638	14.61	4.12	6.01	8.49	6.40	8.83	11.19	?
			21.5	32.4	6.5	0.0	0.0	9.4	3.4	

ened Patterson coefficients. The highest peaks in four of these superposition maps could be interpreted to give two consistent sets of four Cl atoms, as explained above. One of these maps is summarized in Table 2. The letters *A* and *B* refer to the two sets and apply to the rows and columns of the table in which they lie. Each entry in the lower triangular matrix corresponds to the interatomic vector between the atom which defines the row and the atom which defines the column. The two numbers for each pair of atoms (row/column combination) are (on top) the minimum interatomic distance (Å) between the two atoms concerned and (underneath) the value of the sharpened Patterson function at the point which represents the interatomic vector in Patterson space. It will be seen that both the *A* and *B* sets correspond to six acceptable distances and six relatively high Patterson densities, and that the two sets are related by a centre of symmetry. This superposition map was that with the highest correlation coefficient between E_o and E_c (Fujinaga & Read, 1987) calculated for all the atoms shown, *i.e.* the double image plus spurious atoms. Standard automated tangent formula phase expansion from one set of four Cl atoms, followed by iterative *E*-Fourier recycling with peak-list optimization [as incorporated in the program *SHELXS* (Sheldrick 1982, 1990)], led to two virtually complete antibiotic molecules; only the two side chains with partial disorder and high thermal parameters were missing in each molecule. In space groups of higher symmetry than *P*1, it is possible to use the space-group symmetry as an aid to selecting the peaks belonging to one of the two images (Richardson & Jacobson, 1987), and we have recently been able to use this technique for the solution of two small known protein structures (crambin and rubredoxin), for which atomic resolution data are available (Sheldrick, Dauter, Wilson, Hope & Sieker, 1993).

Structure refinement

The structure was refined against F^2 (without applying a threshold) using the new refinement program *SHELXL*93 (Sheldrick, 1995). The convergence of the refinement and the location of solvent and side chains exhibiting high thermal motion was expedited by the use of restraints on the geometric and atomic displacement parameters. The quality and resolution of the data enabled these restraints to be relaxed substantially in the final stages of the refinement, in which all non-H atoms were refined anisotropically by blocked-matrix least squares. The large number of parameters (2603) made full-matrix refinement impractical. For intermediate refinements, we made extensive use of the conjugate-gradient refinement incorporated in *SHELXL*93, which is based on the method of Hendrickson & Konnert (1980); it gives a very stable convergence and is economical in terms of computer time, but does not enable standard deviations to be estimated.

In the final refinement we retained the restraint that the two crystallographically independent but chemically equivalent molecules of the antibiotic have 'similar' 1,2 and 1,3 distances (with e.s.d.'s of 0.03 and 0.05 Å, respectively); this is a very effective way of imposing 'non-crystallographic symmetry', since it leaves the torsion angles free to vary and can accommodate conformational differences. The same distance restraints were employed for the components of the two disordered side chains. We also retained 'rigid-bond' restraints on the differences of the anisotropic displacement components along bonds (1,2) and 1,3 interatomic vectors (Rollett, 1970), except for distances involving the Cl atoms. The corresponding e.s.d.'s were set to 0.01 $Å^2$ for bonded pairs and 0.02 $Å^2$ for 1,3 vectors. For the solvent and the two disordered side chains, the U_{ij} components of (partial) atoms within 1.7 Å of each other were restrained to be equal with e.s.d.'s of 0.05 $Å^2$. The anisotropic displacement parameters of the solvent water molecules were also restrained to be approximately isotropic (with e.s.d.'s of 0.05 $Å^2$). 'Antibumping' restraints were applied to prevent the solvent water atoms from approaching close to other atoms (unless the sum of the occupancies did not exceed unity). These took the form of distance restraints with e.s.d.'s of 0.1 Å and target distances of 2.6 (O···O), 2.7 (O···N), 3.2 (O···C)

and 3.5 Å (O···Cl), which were only applied when the actual distance was less than the target distance. In the final model, the only unreasonably short contact is N208···O24, with a distance of 2.38 (3) Å; however, both these atoms undergo appreciable anisotropic thermal motion (or unresolved disorder), so the average instantaneous N···O distance could be somewhat greater. Attempts to refine group occupancy factors for various combinations of the disordered solvent and side chain atoms resulted in values close to 0.5, but tended to oscillate. Accordingly, the occupancies of all partial atoms were fixed at 0.5, except for the pair of overlapping waters O19 (fixed at 0.8) and O70 (0.2). H atoms were refined using a riding model in which the hydroxy groups were also allowed to rotate about the C—O bonds. No attempt was made to locate the H atoms attached to the solvent waters.

The refinement converged to $wR_2 = \Sigma w(F_o^2 - F_c^2)^2/\Sigma wF_o^4 = 0.1423$ (for all 11 977 data), $R_1 = \Sigma|F_o - F_c|/\Sigma F_o = 0.0536$ for 8949 $F > 4\sigma(F)$ and 0.0802 for all data. The goodness-of-fit $S = [\Sigma w(F_o^2 - F_c^2)^2/(N - M)]^{1/2}$ was 1.041, where N is the number of reflections and M the total number of parameters (2603). A total of 1512 restraints were employed, including three to restrain the floating origin (Flack & Schwarzenbach, 1988). The weighting function employed was $w = [\sigma^2(F^2) + 0.03p + (0.09p)^2]^{-1}$, where $p = [\mathrm{Max}(F_o^2,0) + 2F_c^2]/3$ (Wilson, 1976). Since Friedel opposites had been merged during data processing, the known absolute structure was assumed, and the imaginary parts of the scattering factors were set to zero. The final atomic parameters are presented in Table 3 and selected torsion angles in Table 4. Table 5 gives the hydrogen-bond geometry for those cases in which the H atoms had been included in the refinement as described above. The low e.s.d.'s for the N—H···O angles reflect the fact that these hydrogen positions were effectively determined by the heavy atoms alone, whereas the hydroxy groups were free to rotate and so the O—H···O angles are associated with larger and more variable e.s.d.'s (the e.s.d. of the O—H···O angles passes through a minimum when the H atom lies in the plane defined by the C and two O atoms). At the end of the refinement, a difference electron-density synthesis was performed in which the contributions of the H atoms to F_c were ignored; of the 135 fully occupied H atoms in the two antibiotic molecules, 126 reappeared as peaks within 0.3 Å of their calculated positions. Fig. 1 shows the two independent molecules in similar orientations with the numbering scheme; the solvent water sites are numbered O1–O73, and numbers over 300 refer to alternative positions for the atoms of the two disordered side chains.

Results and discussion

In contrast to the degradation product CDP-1 of vancomycin (Sheldrick, Jones, Kennard, Williams &

Table 3. *Fractional atomic coordinates and equivalent isotropic displacement parameters* (Å^2)

$U_{eq} = (1/3)\Sigma_i\Sigma_j U_{ij} a_i^* a_j^* \mathbf{a}_i.\mathbf{a}_j.$

	x	y	z	U_{eq}
C101	0.5285 (4)	0.7818 (4)	0.9148 (4)	0.0406 (15)
C102	0.4883 (5)	0.7876 (4)	0.8358 (4)	0.0386 (14)
C103	0.4137 (5)	0.8010 (4)	0.8095 (4)	0.0421 (15)
C104	0.3728 (5)	0.8036 (4)	0.8572 (4)	0.0406 (15)
C105	0.4089 (4)	0.7940 (4)	0.9350 (3)	0.0380 (14)
C106	0.4885 (4)	0.7858 (4)	0.9635 (4)	0.0426 (15)
C107	0.5782 (4)	0.7069 (4)	0.7273 (3)	0.0374 (14)
C108	0.5718 (4)	0.6295 (4)	0.6983 (4)	0.0389 (14)
C109	0.5077 (4)	0.5547 (4)	0.6989 (4)	0.0411 (14)
C110	0.4459 (4)	0.5540 (4)	0.7251 (3)	0.0352 (13)
C111	0.4501 (4)	0.6304 (4)	0.7526 (4)	0.0381 (14)
C112	0.5165 (4)	0.7049 (4)	0.7543 (4)	0.0380 (14)
C113	0.5834 (5)	0.4966 (4)	0.5848 (4)	0.049 (2)
C114	0.5852 (5)	0.4220 (5)	0.5763 (4)	0.053 (2)
C115	0.6519 (5)	0.4157 (5)	0.6447 (4)	0.051 (2)
C116	0.7173 (5)	0.4857 (5)	0.7171 (5)	0.056 (2)
C117	0.7130 (5)	0.5592 (4)	0.7243 (4)	0.053 (2)
C118	0.6440 (5)	0.5643 (4)	0.6600 (4)	0.0423 (15)
C119	0.6431 (6)	0.3295 (5)	0.6400 (5)	0.065 (2)
C120	0.5908 (5)	0.2851 (5)	0.6845 (4)	0.057 (2)
C121	0.4884 (5)	0.2661 (5)	0.6421 (4)	0.061 (2)
C122	0.3555 (6)	0.2579 (5)	0.6576 (7)	0.096 (3)
C123	0.3332 (5)	0.3306 (4)	0.6529 (4)	0.053 (2)
C124	0.3702 (4)	0.4714 (4)	0.7216 (3)	0.0333 (13)
C125	0.3622 (4)	0.4905 (4)	0.7998 (4)	0.0389 (14)
C126	0.2796 (5)	0.5368 (4)	0.8543 (3)	0.0386 (14)
C127	0.2232 (5)	0.5795 (4)	0.8189 (3)	0.0390 (14)
C128	0.2922 (4)	0.6824 (4)	0.9576 (3)	0.0384 (14)
C129	0.3564 (5)	0.7805 (4)	0.9827 (3)	0.0385 (14)
C130	0.2317 (5)	0.4788 (4)	0.8921 (3)	0.0416 (15)
C131	0.1397 (5)	0.4070 (5)	0.8425 (4)	0.060 (2)
C132	0.0928 (6)	0.3600 (5)	0.8769 (4)	0.074 (3)
C133	0.1315 (5)	0.3838 (5)	0.9620 (4)	0.058 (2)
C134	0.2228 (5)	0.4557 (4)	1.0151 (4)	0.047 (2)
C135	0.2713 (4)	0.4998 (4)	0.9774 (3)	0.0389 (15)
C136	0.2664 (5)	0.4830 (5)	1.1076 (4)	0.052 (2)
C137	0.3051 (6)	0.4395 (5)	1.1508 (4)	0.056 (2)
C138	0.3442 (6)	0.4611 (5)	1.2356 (4)	0.063 (2)
C139	0.3485 (5)	0.5281 (5)	1.2797 (4)	0.057 (2)
C140	0.3087 (5)	0.5731 (5)	1.2396 (4)	0.053 (2)
C141	0.2683 (5)	0.5512 (4)	1.1532 (4)	0.049 (2)
C142	0.2239 (5)	0.5988 (5)	1.1095 (4)	0.052 (2)
C143	0.2338 (5)	0.6559 (4)	1.0009 (4)	0.046 (2)
C144	0.7398 (4)	0.8171 (4)	0.7929 (4)	0.0423 (15)
C145	0.8434 (5)	0.9080 (5)	0.9316 (4)	0.065 (2)
C146	0.9175 (5)	0.9638 (5)	0.9122 (5)	0.069 (2)
C147	0.9098 (5)	0.9108 (6)	0.8384 (5)	0.074 (2)
C148	0.8091 (5)	0.8650 (5)	0.7661 (4)	0.054 (2)
C149	0.8441 (6)	0.9540 (6)	1.0041 (5)	0.076 (2)
C150	0.7033 (6)	0.3126 (5)	0.8266 (5)	0.070 (2)
C151	0.7655 (6)	0.3739 (5)	0.9159 (5)	0.071 (2)
C152	0.7168 (7)	0.3449 (6)	0.9663 (5)	0.094 (3)
C153	0.7647 (8)	0.3984 (9)	1.0522 (6)	0.119 (4)
C154	0.7149 (10)	0.3605 (12)	1.0977 (8)	0.172 (7)
C155	0.7823 (17)	0.4885 (11)	1.0614 (9)	0.196 (9)
C156	0.9154 (8)	0.4184 (9)	0.9096 (8)	0.113 (4)
C157	0.3139 (8)	0.2069 (7)	0.7073 (10)	0.129 (4)
C158	0.3554 (16)	0.2590 (15)	0.7926 (14)	0.129 (6)
C159	0.3484 (6)	0.9060 (4)	0.9980 (4)	0.054 (2)
C160	0.3425 (5)	0.9130 (5)	1.1228 (4)	0.057 (2)
C161	0.2677 (5)	0.9396 (5)	1.0947 (4)	0.056 (2)
C162	0.2126 (6)	0.9216 (5)	0.9993 (4)	0.062 (2)
C163	0.2811 (6)	0.9388 (5)	0.9650 (5)	0.058 (2)
C164	0.4113 (7)	0.9547 (7)	1.2172 (5)	0.090 (3)
C165	0.1232 (6)	0.8334 (6)	0.9493 (5)	0.084 (3)
C166	0.2498 (7)	1.0536 (6)	1.0727 (5)	0.077 (2)
C167	0.2086 (6)	0.6550 (5)	1.1639 (4)	0.060 (2)
Cl11	0.62332 (14)	0.76521 (15)	0.94981 (12)	0.0710 (6)
Cl12	0.50144 (15)	0.50607 (13)	0.50199 (12)	0.0707 (6)
N101	0.6448 (4)	0.3329 (4)	0.7727 (4)	0.058 (2)
N102	0.4568 (4)	0.2868 (4)	0.6897 (4)	0.064 (2)

Table 3 (*cont.*)

	x	y	z	U_{eq}		x	y	z	U_{eq}
N103	0.3918 (4)	0.4034 (3)	0.7158 (3)	0.0400 (12)	C240	−0.3304 (5)	0.1259 (5)	0.1085 (4)	0.070 (2)
N104	0.2858 (4)	0.4966 (3)	0.7866 (3)	0.0385 (12)	C241	−0.2710 (5)	0.1557 (5)	0.1952 (4)	0.062 (2)
N105	0.2290 (4)	0.6425 (3)	0.8690 (3)	0.0400 (12)	C242	−0.1874 (5)	0.1403 (5)	0.2315 (5)	0.068 (2)
N106	0.2787 (4)	0.6483 (4)	1.0736 (3)	0.0482 (14)	C243	−0.0211 (5)	0.2368 (5)	0.3407 (4)	0.057 (2)
N107	0.8592 (5)	0.3780 (5)	0.9489 (4)	0.084 (2)	C244	0.5089 (4)	0.9090 (4)	0.6608 (4)	0.049 (2)
N108	0.3033 (15)	0.2717 (14)	0.8132 (15)	0.143 (6)	C245	0.6083 (5)	0.9845 (5)	0.8060 (4)	0.059 (2)
N109	0.1899 (6)	0.9896 (5)	0.9996 (4)	0.078 (2)	C246	0.6880 (5)	1.0457 (5)	0.7943 (5)	0.065 (2)
N110	0.3042 (5)	1.0300 (4)	1.1249 (4)	0.070 (2)	C247	0.6808 (5)	1.0025 (5)	0.7167 (5)	0.068 (2)
O101	0.5262 (3)	0.7836 (3)	0.7844 (3)	0.0444 (10)	C248	0.5827 (5)	0.9653 (5)	0.6417 (5)	0.058 (2)
O102	0.6450 (3)	0.7813 (3)	0.7273 (2)	0.0398 (10)	C249	0.6044 (6)	1.0192 (5)	0.8820 (5)	0.066 (2)
O103	0.6350 (3)	0.6347 (3)	0.6710 (3)	0.0500 (11)	C250	−0.1785 (6)	0.8490 (6)	0.4672 (5)	0.069 (2)
O104	0.7357 (4)	0.3398 (4)	0.6804 (4)	0.083 (2)	C251	−0.2074 (7)	0.8129 (7)	0.3773 (6)	0.096 (3)
O105	0.4382 (4)	0.2332 (5)	0.5662 (3)	0.104 (2)	C252	−0.2990 (14)	0.7246 (10)	0.3349 (9)	0.216 (9)
O106	0.2598 (5)	0.3164 (4)	0.5944 (4)	0.109 (3)	C253	−0.3288 (19)	0.6563 (14)	0.3558 (16)	0.140 (8)
O107	0.4247 (4)	0.5045 (3)	0.8690 (3)	0.0619 (13)	C254	−0.3483 (18)	0.6583 (16)	0.4235 (16)	0.127 (7)
O108	0.1669 (4)	0.5521 (3)	0.7425 (2)	0.0635 (14)	C255	−0.4105 (25)	0.5733 (18)	0.2836 (20)	0.199 (16)
O109	0.2969 (3)	0.8157 (3)	0.9645 (3)	0.0460 (11)	C353	−0.3263 (22)	0.6631 (18)	0.2660 (20)	0.206 (12)
O110	0.0829 (5)	0.3385 (4)	0.9970 (4)	0.088 (2)	C354	−0.2610 (29)	0.6354 (28)	0.2618 (30)	0.253 (18)
O111	0.3027 (5)	0.3739 (4)	1.1048 (3)	0.078 (2)	C355	−0.4222 (24)	0.5820 (19)	0.2383 (23)	0.222 (18)
O112	0.3898 (5)	0.5482 (4)	1.3639 (3)	0.081 (2)	C256	−0.1470 (13)	0.9585 (10)	0.3707 (10)	0.178 (7)
O113	0.1509 (4)	0.6362 (4)	0.9685 (3)	0.0653 (14)	C257	−0.1550 (7)	0.6081 (7)	0.6174 (8)	0.105 (3)
O114	0.7514 (3)	0.8724 (3)	0.8603 (3)	0.0576 (13)	C258	−0.1778 (9)	0.5699 (9)	0.5323 (10)	0.138 (5)
O115	1.0108 (4)	1.0023 (5)	0.9818 (4)	0.116 (3)	C259	0.2472 (5)	0.3214 (5)	0.3578 (4)	0.051 (2)
O116	0.9766 (5)	0.9677 (4)	0.8183 (5)	0.117 (3)	C260	0.1369 (6)	0.1971 (5)	0.2352 (4)	0.060 (2)
O117	0.8032 (4)	0.8101 (4)	0.7014 (3)	0.070 (2)	C261	0.1842 (5)	0.1481 (5)	0.2713 (4)	0.059 (2)
O118	0.8297 (5)	1.0194 (4)	0.9900 (4)	0.090 (2)	C262	0.2444 (6)	0.1824 (5)	0.3671 (4)	0.061 (2)
O119	0.7079 (5)	0.2490 (4)	0.8080 (4)	0.098 (2)	C263	0.3019 (5)	0.2810 (5)	0.3981 (4)	0.060 (2)
O120	0.4430 (14)	0.2805 (17)	0.8473 (15)	0.176 (9)	C264	0.0963 (7)	0.1732 (6)	0.1419 (4)	0.084 (3)
O121	0.3996 (3)	0.9366 (3)	1.0856 (3)	0.0549 (12)	C265	0.1872 (7)	0.1482 (6)	0.4092 (5)	0.076 (2)
O122	0.2052 (5)	0.8966 (4)	1.1235 (4)	0.079 (2)	C266	0.3201 (7)	0.1415 (6)	0.3101 (5)	0.079 (2)
O123	0.2534 (7)	1.1233 (5)	1.0894 (4)	0.116 (3)	C267	−0.1951 (7)	0.0734 (6)	0.1685 (5)	0.086 (3)
O124	0.1288 (5)	0.6220 (4)	1.1594 (4)	0.086 (2)	Cl21	0.2104 (2)	0.6680 (2)	0.37392 (13)	0.0857 (7)
O125	0.2737 (5)	0.7288 (4)	1.2050 (3)	0.082 (2)	Cl22	0.34348 (15)	0.9851 (2)	0.80352 (13)	0.0767 (6)
C358	0.3822 (24)	0.2381 (20)	0.7964 (16)	0.209 (13)	N201	−0.1016 (4)	0.8499 (4)	0.5237 (4)	0.063 (2)
O320	0.4595 (17)	0.3143 (14)	0.8455 (12)	0.156 (7)	N202	−0.0663 (5)	0.7585 (4)	0.6237 (4)	0.063 (2)
N308	0.4149 (26)	0.1854 (21)	0.8022 (24)	0.275 (19)	N203	0.0435 (4)	0.6819 (3)	0.6200 (3)	0.0405 (12)
C201	0.2365 (5)	0.5985 (4)	0.4178 (4)	0.048 (2)	N204	0.0522 (4)	0.4999 (3)	0.5599 (3)	0.0396 (12)
C202	0.3101 (4)	0.6285 (4)	0.4986 (4)	0.0423 (15)	N205	0.1028 (4)	0.3498 (4)	0.4767 (3)	0.0455 (13)
C203	0.3346 (5)	0.5746 (4)	0.5313 (4)	0.046 (2)	N206	−0.0964 (4)	0.2225 (4)	0.2713 (3)	0.059 (2)
C204	0.2832 (4)	0.4891 (4)	0.4865 (4)	0.044 (2)	N207	−0.2281 (7)	0.8712 (6)	0.3344 (5)	0.107 (3)
C205	0.2036 (4)	0.4542 (4)	0.4065 (3)	0.0429 (15)	N208	−0.1901 (15)	0.4932 (8)	0.5184 (15)	0.273 (11)
C206	0.1825 (5)	0.5112 (4)	0.3719 (4)	0.050 (2)	N209	0.3098 (5)	0.1513 (5)	0.3777 (4)	0.074 (2)
C207	0.3423 (4)	0.8266 (4)	0.5983 (4)	0.0390 (14)	N210	0.2528 (5)	0.1503 (4)	0.2503 (4)	0.068 (2)
C208	0.2904 (4)	0.8531 (4)	0.6213 (4)	0.0411 (14)	O201	0.3601 (3)	0.7152 (3)	0.5477 (3)	0.0470 (11)
C209	0.2120 (5)	0.7970 (4)	0.6255 (4)	0.0439 (15)	O202	0.4181 (3)	0.8848 (3)	0.5929 (3)	0.0454 (11)
C210	0.1865 (4)	0.7115 (4)	0.6081 (4)	0.0389 (14)	O203	0.3195 (3)	0.9396 (3)	0.6366 (3)	0.0522 (11)
C211	0.2363 (4)	0.6841 (4)	0.5834 (4)	0.0382 (14)	O204	−0.0084 (5)	1.0254 (4)	0.5919 (5)	0.093 (2)
C212	0.3108 (5)	0.7400 (4)	0.5752 (4)	0.0404 (14)	O205	0.0203 (4)	0.8732 (4)	0.7399 (3)	0.0689 (15)
C213	0.2560 (5)	0.9801 (4)	0.7138 (4)	0.052 (2)	O206	0.0669 (5)	0.6746 (5)	0.7455 (3)	0.088 (2)
C214	0.1847 (5)	0.9910 (5)	0.7156 (5)	0.057 (2)	O207	−0.0048 (4)	0.5623 (3)	0.4735 (3)	0.0613 (13)
C215	0.1121 (5)	0.9842 (5)	0.6432 (5)	0.057 (2)	O208	0.1445 (4)	0.4182 (3)	0.6047 (3)	0.0604 (13)
C216	0.1156 (6)	0.9714 (5)	0.5705 (5)	0.064 (2)	O209	0.1810 (3)	0.3113 (3)	0.3840 (2)	0.0476 (11)
C217	0.1870 (5)	0.9598 (5)	0.5693 (4)	0.055 (2)	O210	−0.3212 (5)	0.1091 (5)	0.3560 (4)	0.135 (3)
C218	0.2545 (5)	0.9606 (4)	0.6409 (4)	0.048 (2)	O211	−0.3949 (5)	0.2365 (6)	0.2633 (4)	0.104 (2)
C219	0.0263 (6)	0.9836 (5)	0.6426 (5)	0.067 (2)	O212	−0.4710 (4)	0.1046 (5)	−0.0085 (3)	0.093 (2)
C220	−0.0591 (5)	0.8921 (5)	0.6117 (4)	0.056 (2)	O213	−0.0176 (4)	0.1815 (4)	0.3693 (3)	0.076 (2)
C221	−0.0299 (5)	0.8412 (5)	0.6645 (4)	0.053 (2)	O214	0.5181 (3)	0.9562 (3)	0.7315 (3)	0.0533 (12)
C222	−0.0599 (6)	0.6987 (5)	0.6669 (5)	0.067 (2)	O215	0.7811 (4)	1.0790 (4)	0.8640 (4)	0.086 (2)
C223	0.0245 (6)	0.6866 (5)	0.6812 (4)	0.056 (2)	O216	0.7534 (5)	1.0617 (5)	0.7040 (5)	0.099 (2)
C224	0.1041 (4)	0.6491 (4)	0.6177 (4)	0.0378 (14)	O217	0.5765 (4)	0.9171 (4)	0.5725 (4)	0.087 (2)
C225	0.0442 (4)	0.5656 (4)	0.5437 (3)	0.0398 (15)	O218	0.6067 (5)	1.0956 (4)	0.8879 (4)	0.091 (2)
C226	0.0225 (4)	0.4258 (4)	0.4942 (4)	0.0417 (15)	O219	−0.2226 (4)	0.8764 (4)	0.4849 (4)	0.088 (2)
C227	0.0949 (4)	0.3983 (4)	0.5284 (3)	0.043 (2)	O220	−0.1830 (7)	0.6062 (7)	0.4817 (6)	0.159 (4)
C228	0.0588 (5)	0.3309 (4)	0.3865 (3)	0.047 (2)	O221	0.2003 (3)	0.2872 (3)	0.2698 (3)	0.0545 (12)
C229	0.1360 (5)	0.3598 (4)	0.3618 (4)	0.047 (2)	O222	0.1110 (5)	0.0608 (3)	0.2406 (4)	0.080 (2)
C230	−0.0749 (5)	0.3489 (4)	0.4608 (4)	0.049 (2)	O223	0.3797 (5)	0.1271 (5)	0.3043 (4)	0.105 (2)
C231	−0.0956 (6)	0.3016 (6)	0.5113 (5)	0.080 (3)	O224	−0.2528 (6)	−0.0048 (4)	0.1530 (5)	0.120 (3)
C232	−0.1782 (7)	0.2238 (7)	0.4769 (5)	0.101 (4)	O225	−0.1485 (5)	0.0980 (5)	0.1339 (5)	0.129 (3)
C233	−0.2407 (6)	0.1891 (5)	0.3926 (5)	0.080 (3)	O1	0.6003 (7)	0.4555 (6)	0.8440 (5)	0.144 (4)
C234	−0.2240 (5)	0.2318 (5)	0.3402 (4)	0.056 (2)	O2	−0.0339 (6)	0.7440 (5)	0.4676 (4)	0.107 (2)
C235	−0.1415 (4)	0.3135 (4)	0.3767 (4)	0.048 (2)	O3	0.4770 (5)	0.7015 (6)	1.1218 (6)	0.141 (3)
C236	−0.2897 (5)	0.1960 (5)	0.2481 (4)	0.057 (2)	O4	−0.0606 (5)	0.3868 (5)	0.2403 (4)	0.105 (2)
C237	−0.3735 (5)	0.1990 (6)	0.2135 (5)	0.070 (2)	O5	1.0079 (5)	0.4566 (5)	1.1177 (4)	0.113 (2)
C238	−0.4338 (6)	0.1669 (6)	0.1300 (5)	0.073 (2)	O6	−0.2740 (14)	0.8390 (10)	0.1690 (7)	0.245 (8)
C239	−0.4118 (5)	0.1345 (5)	0.0772 (4)	0.068 (2)	O7	0.3241 (27)	0.3441 (23)	0.9563 (21)	0.221 (12)

Table 3 (*cont.*)

	x	y	z	U_{eq}
O8	−0.4013 (11)	0.8609 (13)	0.2805 (12)	0.259 (9)
O9	0.1215 (21)	0.1912 (19)	0.7556 (25)	0.247 (14)
O10	−0.1904 (14)	1.0335 (10)	0.5858 (12)	0.235 (7)
O11	0.1020 (5)	0.3643 (5)	1.1541 (4)	0.093 (2)
O12	−0.3468 (14)	0.0149 (14)	0.4513 (12)	0.304 (11)
O13	0.3932 (9)	0.2992 (7)	1.1885 (7)	0.165 (4)
O14	−0.3388 (31)	0.2976 (26)	0.4300 (17)	0.248 (14)
O15	0.4650 (5)	0.7200 (5)	1.4395 (4)	0.110 (2)
O16	−0.0485 (11)	0.0110 (14)	0.2461 (12)	0.266 (9)
O17	1.0714 (6)	0.9409 (6)	1.1051 (5)	0.131 (3)
O18	0.4624 (17)	0.9277 (15)	0.4304 (9)	0.302 (10)
O19	0.6584 (7)	0.8195 (7)	0.5581 (5)	0.111 (3)
O20	−0.0437 (21)	0.1830 (20)	0.8867 (20)	0.250 (15)
O21	−0.1069 (9)	0.2408 (8)	0.9516 (8)	0.091 (4)
O22	−0.5773 (9)	0.1896 (8)	−0.0474 (7)	0.177 (4)
O23	0.8110 (12)	0.2170 (9)	0.9747 (11)	0.116 (5)
O24	−0.2043 (23)	0.3801 (21)	0.5724 (20)	0.211 (11)
O25	0.4887 (7)	0.1136 (6)	0.7212 (8)	0.163 (4)
O26	−0.0182 (6)	0.5909 (6)	0.8337 (5)	0.137 (3)
O27	0.9222 (7)	0.2491 (7)	0.1169 (6)	0.156 (4)
O28	0.6472 (28)	0.5964 (24)	0.9313 (25)	0.302 (21)
O29	0.7480 (24)	0.6538 (17)	0.9121 (11)	0.191 (10)
O30	0.4597 (7)	0.8007 (7)	0.3162 (7)	0.167 (4)
O31	0.3982 (15)	0.0461 (11)	0.5349 (12)	0.245 (7)
O32	0.9004 (17)	0.4478 (13)	0.6769 (13)	0.140 (7)
O33	0.7358 (19)	0.1913 (13)	0.6608 (16)	0.170 (9)
O34	0.6962 (19)	0.1716 (13)	0.6119 (14)	0.160 (9)
O35	0.2330 (15)	0.8351 (10)	0.2696 (11)	0.244 (7)
O36	0.2162 (14)	0.1089 (10)	0.8925 (11)	0.232 (6)
O37	0.0624 (10)	1.1598 (10)	0.5245 (8)	0.242 (8)
O38	0.5239 (10)	0.5984 (11)	0.0442 (8)	0.224 (6)
O39	0.1254 (14)	0.1769 (9)	0.9680 (8)	0.236 (7)
O40	0.0564 (15)	0.7202 (14)	0.0833 (14)	0.299 (10)
O41	0.9172 (13)	0.5207 (9)	0.3008 (6)	0.236 (7)
O42	0.5898 (7)	0.9496 (8)	0.1776 (7)	0.169 (4)
O43	−0.4232 (23)	0.2289 (27)	0.4074 (16)	0.228 (13)
O44	0.1239 (15)	0.2620 (15)	0.6664 (13)	0.167 (8)
O45	1.1388 (29)	0.9338 (20)	0.3152 (28)	0.462 (19)
O46	0.9474 (13)	1.1144 (13)	0.7922 (13)	0.137 (6)
O47	1.0342 (36)	1.1249 (31)	0.8171 (28)	0.320 (18)
O48	1.0165 (18)	0.6522 (17)	0.2403 (13)	0.162 (8)
O49	−0.2937 (28)	0.4179 (16)	0.3008 (23)	0.227 (12)
O50	−0.4100 (43)	0.3809 (34)	0.2134 (42)	0.335 (23)
O51	0.5372 (25)	0.4301 (29)	0.9483 (20)	0.262 (15)
O52	0.5978 (29)	1.1090 (28)	0.4980 (24)	0.306 (21)
O53	−0.2384 (36)	0.4969 (38)	0.3176 (33)	0.304 (17)
O54	0.4138 (25)	0.4094 (20)	1.0175 (18)	0.193 (10)
O55	0.9037 (12)	0.2947 (11)	0.6920 (10)	0.238 (7)
O56	0.0856 (11)	0.7658 (11)	0.4042 (9)	0.234 (7)
O57	0.9652 (13)	0.1925 (12)	0.6768 (12)	0.267 (8)
O58	0.8991 (11)	0.6147 (13)	0.9270 (9)	0.245 (7)
O59	0.2485 (20)	0.8878 (15)	0.4192 (13)	0.320 (11)
O60	−0.4924 (20)	0.3431 (18)	0.1026 (23)	0.205 (11)
O61	0.5240 (15)	0.3549 (18)	0.3624 (11)	0.311 (11)
O62	0.7340 (23)	0.6900 (20)	0.0884 (18)	0.381 (14)
O63	0.9481 (27)	0.6496 (22)	0.2575 (21)	0.253 (14)
O64	−0.0147 (23)	0.8777 (20)	0.3310 (19)	0.367 (13)
O65	0.4818 (32)	1.0848 (31)	0.4393 (23)	0.291 (18)
O66	0.8295 (39)	0.6664 (41)	1.2418 (36)	0.360 (25)
O67	−0.1672 (45)	0.5849 (43)	0.3455 (42)	0.378 (24)
O68	0.9375 (50)	0.7346 (39)	0.1679 (41)	0.402 (31)
O69	0.9485 (30)	0.7802 (33)	0.0964 (31)	0.304 (19)
O70	0.6607 (41)	0.7251 (42)	0.5373 (35)	0.181 (22)
O71	0.8686 (38)	0.8183 (36)	0.1094 (38)	0.383 (28)
O72	1.0487 (30)	0.7051 (26)	0.2038 (27)	0.288 (17)
O73	0.9659 (19)	0.4629 (18)	0.7227 (19)	0.196 (10)

Table 4. *Selected torsion angles* (°)

	Molecule *A*	Molecule *B*
Hexose linkage		
C(108)—C(107)—O(102)—C(144)	−78.0 (6)	104.7 (6)
C(107)—O(102)—C(144)—C(148)	151.1 (5)	174.8 (5)
Vancosamine linkage		
C(128)—C(129)—O(109)—C(159)	169.3 (5)	173.1 (5)
C(129)—O(109)—C(159)—C(163)	171.3 (5)	169.4 (5)
Aromatic ether linkage		
C(117)—C(118)—O(103)—C(108)	−90.9 (7)	−92.0 (7)
C(118)—O(103)—C(108)—C(109)	−12.6 (8)	−11.4 (8)
C(103)—C(102)—O(101)—C(112)	−115.4 (6)	−106.5 (7)
C(102)—O(101)—C(112)—C(111)	19.6 (8)	23.8 (8)
Peptide ψ		
N(107)—C(151)—C(150)—N(101)	−143.4 (7)	−135.0 (8)
N(101)—C(120)—C(121)—N(102)	−6.6 (10)	−15.0 (9)
N(102)—C(122)—C(123)—N(103)	−42.8 (12)	−40.5 (10)
N(103)—C(124)—C(125)—N(104)	−133.2 (5)	−130.1 (6)
N(104)—C(126)—C(127)—N(105)	−159.6 (6)	−160.0 (6)
N(105)—C(128)—C(143)—N(106)	146.2 (6)	143.6 (6)
Peptide ω		
C(151)—C(150)—N(101)—C(120)	172.6 (7)	172.2 (7)
C(120)—C(121)—N(102)—C(122)	−168.8 (7)	−168.0 (6)
C(122)—C(123)—N(103)—C(124)	−172.2 (7)	−163.9 (6)
C(124)—C(125)—N(104)—C(126)	−162.6 (5)	−162.1 (5)
C(126)—C(127)—N(105)—C(128)	6.0 (9)	11.5 (10)
C(128)—C(143)—N(106)—C(142)	−161.0 (6)	−165.2 (6)
Peptide ϕ		
C(150)—N(101)—C(120)—C(121)	138.2 (7)	138.2 (7)
C(121)—N(102)—C(122)—C(123)	−111.3 (9)	−96.7 (8)
C(123)—N(103)—C(124)—C(125)	118.2 (7)	113.9 (7)
C(125)—N(104)—C(126)—C(127)	146.4 (6)	141.2 (6)
C(127)—N(105)—C(128)—C(143)	−109.6 (7)	−110.3 (7)
C(143)—N(106)—C(142)—C(167)	−88.4 (8)	−89.5 (9)

Smith, 1978), ureido-balhimycin has the two Cl atoms on opposite sides of the aromatic core, and contains asparagine rather than isoasparagine, exactly as shown for vancomycin itself in NMR studies (Williamson & Williams, 1981; Harris, Kopecka & Harris, 1983). This rearrangement increases the ring size by one atom, making it possible for the chlorophenyl moiety to rotate about its axis. The NMR studies show that this rotation is slow in CDP-1, but cannot take place at all in vancomycin (and hence balhimycin). In vancomycin, the vancosamine is linked to glucose, whereas in balhimycin a C4-oxidized vancosamine is linked to a benzylic hydroxy group. This 4-oxo-vancosaminyl residue has reacted with potassium isocyanate to give a cyclic ureido derivative, which is derived from the epi form of the vancosamine saccharide (Gauze, Brazhnikova, Laiko, Sveshnikova, Preobrazhenskaya, Fedorova, Borisova, Tolstykh, Yurina, Pokras, Goldberg, Malkova & Stepanova, 1987; Tsuji, Kobayashi, Kamigauchi, Yoshimura & Terui, 1988). This 4-keto-vancosamine may be regarded as the 'missing link' between vancosamine and its epi form. It is probable that balhimycin has the ketone hydrate structure in solution (Fehlhaber, Kogler & Vértesy, 1991).

Fig. 2 shows a least-squares fit of the two independent antibiotic molecules, in which all atoms except the two carboxyl oxygens and the glucose, ureido-vancosamine,

aparagine and leucine side chains were fitted (*i.e.* including C167, O102, O109, C157 and N101, but not the atoms further out along these side chains). The r.m.s. deviation of the fitted atoms was 0.36 Å. It will be seen that the glucose substituent has been rotated by *ca* 180°, but that the rest of the two molecules have fairly similar conformations; this is confirmed by inspection of the torsion angles given in Table 4. The two molecules in the cell are linked together in an antiparallel arrangement by the four amide-NH···carbonyl oxygen hydrogen bonds N104···O208, N105···O206, N204···O108 and N205···O106, as shown in Fig. 3. An approximate local twofold axis relates the two antibiotic molecules, but is strongly violated by the two glucose units. There are also the possible hydrogen bonds O118···O215 between the two glucose units and N209···O105 between the vancosamine nitrogen and a peptide carbonyl; however, the distance related to the latter by the approximate twofold axis (N109···O205) is longer [4.216 (12) Å]. In the free balhimycin, N109 and N209 are free $—NH_2$ or $—NH_3^+$ groups rather than —NH— groups of cyclic

Table 5. *Hydrogen-bonding geometry* (Å, °)

D	*A*	*D*···*A*	*D*—H···*A*
N101	O1	3.043 (10)	164.9 (4)
N102	O1	3.138 (11)	148.8 (3)
N103	O1	3.128 (10)	165.7 (3)
N104	O208	2.993 (7)	165.4 (2)
N105	O206	3.230 (8)	162.2 (3)
N106	O3	2.939 (10)	158.4 (3)
N107	O5	2.845 (10)	155.8 (3)
N107	O21^{i}	2.842 (15)	152.2 (4)
N108	O7	2.67 (4)	158.0 (12)
N108	O9	2.58 (4)	137.5 (15)
N110	O223^{ii}	3.052 (10)	131.7 (3)
N201	O2	2.993 (10)	170.1 (3)
N202	O2	3.230 (9)	133.7 (2)
N203	O2	3.217 (9)	172.7 (2)
N204	O108	2.968 (7)	158.9 (2)
N205	O106	3.144 (8)	158.8 (2)
N206	O4	3.010 (10)	159.2 (2)
N207	O6	2.801 (15)	163.3 (5)
N208	O24	2.39 (3)	142.0 (13)
N209	O105	3.062 (9)	129.0 (3)
N210	O123^{iii}	3.026 (9)	155.7 (2)
O110	O20	2.65 (3)	144 (11)
O111	O13	2.703 (11)	156 (9)
O112	O15	2.777 (11)	174 (11)
O115	O17	2.730 (13)	155 (2)
O118	O225^{iv}	2.715 (9)	137 (11)
O122	O17^{v}	2.749 (10)	169 (6)
O204	O37	2.966 (13)	120 (7)
O210	O12	2.68 (2)	136 (15)
O211	O14	2.80 (3)	123 (7)
O212	O22	2.875 (13)	177 (12)
O217	O18	2.72 (2)	170 (12)
O218	O212^{iv}	2.852 (10)	137 (11)
O222	O16	2.660 (14)	157 (5)

Symmetry codes: (i) $x+1, y, z$; (ii) $x, y+1, z+1$; (iii) $x, y-1, z-1$; (iv) $x+1, y+1, z+1$; (v) $x-1, y, z$.

ureas, and may well be able to form stronger hydrogen bonds to the other antibiotic molecule, stabilizing the dimer. It is likely that these dimers would persist in solution. As a result of the dimer formation, most of the other atoms which could take part in hydrogen bonding are on the surface of the dimer and take part in interactions (shown in Table 4) with the solvent and

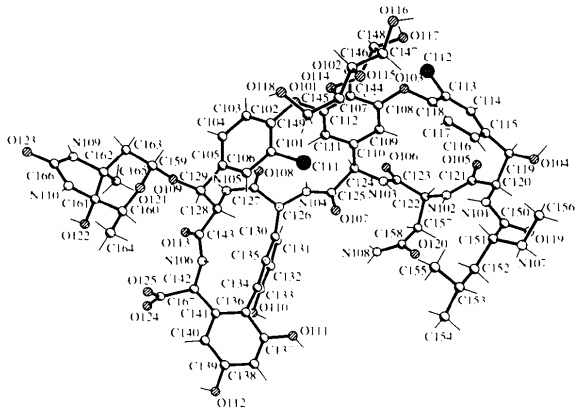

(*A*)

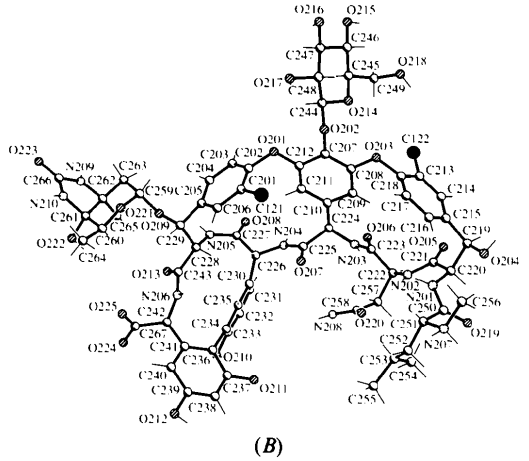

(*B*)

Fig. 1. The two independent molecules (*A* and *B*) of ureido-balhimycin, showing the numbering scheme. For clarity, only one component of each of the two disordered side chains is shown in this and subsequent figs.

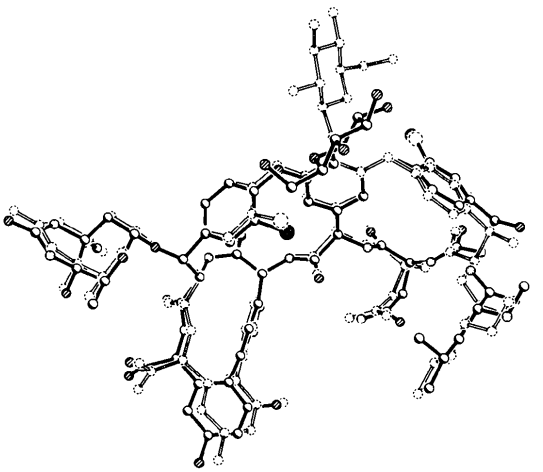

Fig. 2. Least-squares fit of the two independent molecules.

with other dimer units; in fact, only two of the polar H atoms of the antibiotic molecules do not appear to form strong hydrogen bonds (attached to N109 and N208). 57 of the 73 water sites are in the first hydration shell and the remaining 16 (with an occupancy sum of 12) are in the second shell. Fig. 3 illustrates how closely the two monomers fit together, with, for example, one of the Cl atoms projecting into a hole in the other monomer.

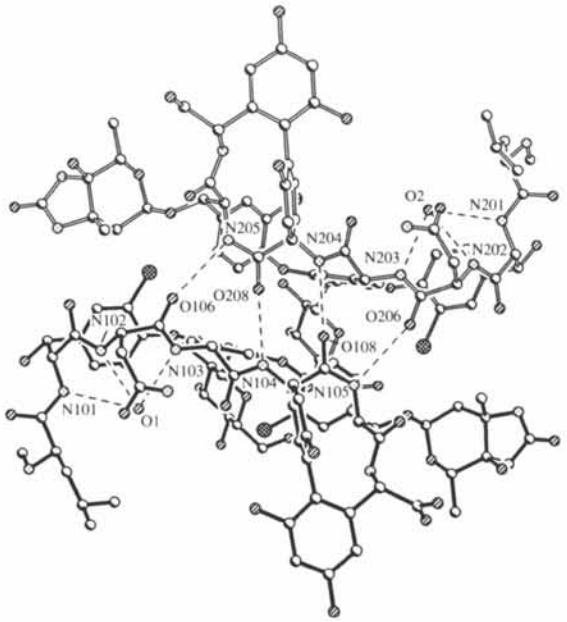

Fig. 3. The ureido-balhimycin dimer, showing key hydrogen bonds.

Recently Gerhard, Mackay, Maplestone & Williams (1993) have presented convincing NMR evidence for the formation of such dimers in aqueous solutions of eremomycin, vancomycin, ristocetin and related glycopeptide antibiotics, and their proposed scheme of hydrogen bonds linking the two monomer units is in close agreement with the pattern observed here for balhimycin.

Fig. 3 also shows the two embedded hydrogen-bonded water molecules O1 and O2. These molecules are surrounded by hydrophilic groups and are each at hydrogen-bonding distances from three peptide nitrogens, which may also add some rigidity to the peptide backbone conformation. Williams & Butcher (1981) and Williams, Williamson, Butcher & Hammond (1983) have shown by NMR that the same three amide NH groups in vancomycin hydrogen bond to the C-terminal carboxyl of the peptide Ac-D-Ala-D-Ala, so this region is believed to serve as a pocket for cell-wall protein which interacts with vancomycin. The arrangement of the various groups around this site suggests that the conformation observed here for balhimycin is close to that of the 'binding pocket' proposed by Williams & Butcher (1981) and Williams, Williamson, Butcher & Hammond (1983); in CDP-1, quite a different conformation was found as a result of the increased ring size (Sheldrick, Jones, Kennard, Williams & Smith, 1978). When the C-terminus of the peptide is anchored in this binding pocket, the phenolic hydroxyl groups of the diphenyl unit would be well placed to attack the peptide chain a few residues back from the C-terminus. The binding pockets of the two molecules which constitute the dimer can be seen to the upper right and lower left in the space-filling

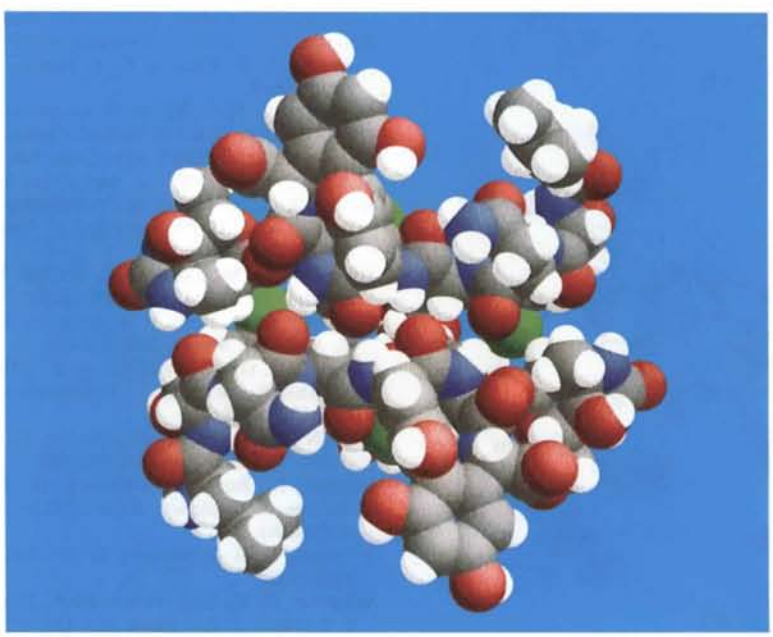

Fig. 4. Space-filling view of the ureido-balhimycin dimer. The cleft dividing the two components of the dimer bisects the picture horizontally. The presumed 'peptide binding pockets' can be seen to the upper right and lower left.

model shown in Fig. 4. Since dimer formation in no way hinders access to these pockets, it is possible that the biologically active form of the antibiotic retains the dimeric structure, *i.e.* that the dimer formation is not simply a way of improving the transport of the antibiotic through aqueous medium. Gerhard, Mackay, Maplestone & Williams (1993) discussed the possibility that dimerization is implicated in antibiotic action, and that natural selection has favoured structural features that promote dimerization.

The displacement ellipsoids (Fig. 5) for the two antibiotic molecules are in general relatively small for a structure of this type, indicating that the confomation of the cyclic systems is relatively rigid, but the asparagine and leucine side chains exhibit considerable thermal motion in both molecules, and two of these side chains are also disordered (for clarity, only one component of each disordered side chain is shown in the figures). These side chains could well constitute the 'flaps' of the binding pocket, and would move to let the substrate molecules in and out.

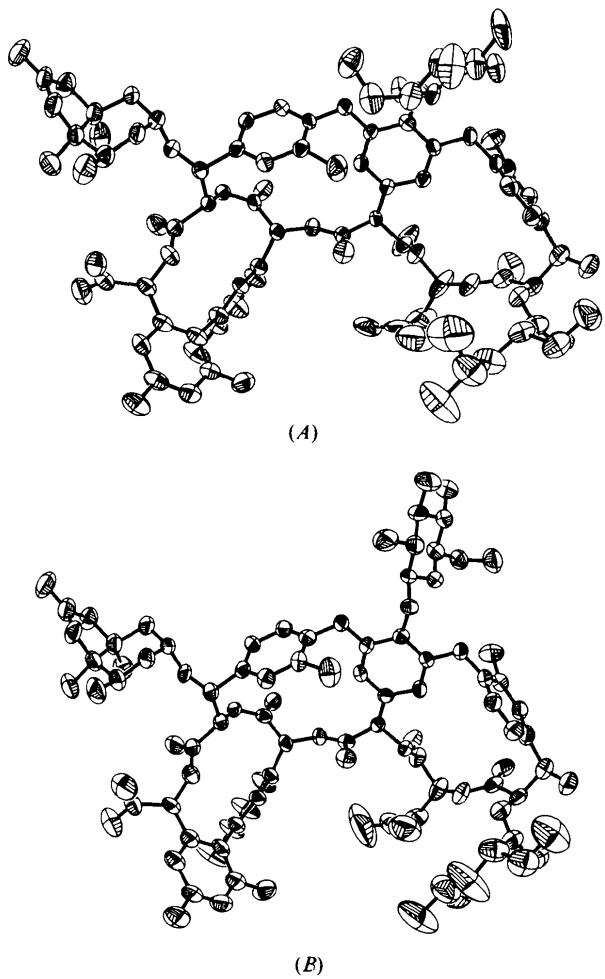

Fig. 5. Anisotropic displacement parameter ellipsoids at 50% probability of the two independent molecules (*A* and *B*). H atoms have been omitted for clarity.

GMS is grateful to the Fonds de: Chemischen Industrie and to the Leibniz Programme of the Deutsche Forschungsgemeinschaft for financial support.

References

BOYCE, J. M. (1989). *Dis. Clin. North Am.* **3**, 901–904.

BUERGER, M. J. (1959). *Vector Space*, ch. 11. New York: Wiley.

FEHLHABER, H. W., KOGLER, H. & VÉRTESY, L. (1991). Personal communication.

FLACK, H. D. & SCHWARZENBACH, D. (1988). *Acta Cryst.* A**44**, 499–506.

FUJINAGA, M. & READ, R. J. (1987). *J. Appl. Cryst.* **20**, 517–521.

GAUZE, G. F., BRAZHNIKOVA, M. G., LAIKO, A. V., SVESHNIKOVA, M. A., PREOBRAZHENSKAYA, T. P., FEDOROVA, G. B., BORISOVA, V. N., TOLSTYKH, I. V., YURINA, M. S., POKRAS, L. S., GOLDBERG, L. E., MALKOVA, I. V. & STEPANOVA, E. S. (1987). *Antibiotiki*, **32**, 571–576.

GERHARD, U., MACKAY, J. P., MAPLESTONE, R. A. & WILLIAMS, D. H. (1993). *J. Am. Chem. Soc.* **115**, 232–237.

HARRIS, C. M., KOPECKA, H. & HARRIS, TH. M. (1983). *J. Am. Chem. Soc.* **105**, 6915–6922.

HENDRICKSON, W. A. & KONNERT, J. H. (1980). In *Computing in Crystallography*, edited by R. DIAMOND, S. RAMASESHAN & K. VENKATESAN, pp. 13.01–13.25. Bangalore: IUCr and Indian Academy of Sciences.

MIYAHARA, J. & KATO, H. (1984). *Jpn. Soc. Appl. Phys.* **53**, 884–890.

NADKARNI, S. R., CHATTERJEE, S., PATEL, M. V., DESIKAN, K. R., VIJAYAKUMAR, E. K. S., GANGULI, B. N., BLUMBACH, J., FEHLHABER, H. W. & KOGLER, H. (1990). A Novel Antibiotic, Balhimycin, a Process for its Production and its use as a Pharmaceutical. Patent EP 0468504A1.

NAGARAJAN, R. (1991). *Antimicrob. Agents Chemother.* **35**, 605–609.

NAGARAJAN, R., MERKEL, K. E., MICHEL, K. H., HIGGINS, H. M. JR., HOEHN, M. M., HUNT, A. H., JONES, N. D., OCCOLOWITZ, J. L., SCHABEL, A. A. & SWARTZENDRUBER, J. K. (1988). *J. Am. Chem. Soc.* **110**, 7896–7897.

RICHARDSON, J. W. & JACOBSON, R. A. (1987). In *Patterson and Pattersons*, edited by J. P. GLUSKER, B. K. PATTERSON & M. ROSSI, pp. 310–317. Oxford: Oxford Univ. Press.

ROLLETT, J. S. (1970). In *Crystallographic Computing*, edited by F. R. AHMED, S. R. HALL & C. P. HUBER, pp. 167–181. Copenhagen: Munksgaard.

SHELDRICK, G. M. (1982). In *Computational Crystallography*, edited by D. SAYRE, pp. 506–514. Oxford: Clarendon Press.

SHELDRICK, G. M. (1990). *Acta Cryst.* A**46**, 467–473.

SHELDRICK, G. M. (1995). *J. Appl. Cryst.* In preparation.

SHELDRICK, G. M. (1992). In *Crystallographic Computing* 5, edited by D. MORAS, A. D. PODJARNY & J. C. THIERRY, pp. 145–157. Oxford: Oxford Univ. Press.

SHELDRICK, G. M., DAUTER, Z., WILSON, K. S., HOPE, H. & SIEKER, L. C. (1993). *Acta Cryst.* D**49**, 18–23.

SHELDRICK, G. M., JONES, P. G., KENNARD, O., WILLIAMS, D. H. & SMITH, G. A. (1978). *Nature*, **271**, 223–225.

STARK, G. R. (1965). *Biochemistry*, **4**, 1030–1036.

TAKAHASHI, K., MIYAHARA, J. & SHIBAHARA, Y. (1985). *J. Electrochem. Soc.* **132**, 1492.

TSUJI, N., KOBAYASHI, M., KAMIGAUCHI, T., YOSHIMURA, Y. & TERUI, Y. (1988). *J. Antibiotics*, **XLI**, 819–822.

VÉRTESY, L., BETZ, J., FEHLHABER, H. W. & LIMBERT, M. (1992). Balhimycin-Abgeleitete Glykopeptidische Antibiotika. Patent EP-0521408A1.

WILLIAMS, D. H. & BUTCHER, D. W. (1981). *J. Am. Chem. Soc.* **103**, 5697–5700.

WILLIAMS, D. H., WILLIAMSON, M. P., BUTCHER, D. W. & HAMMOND, S. J. (1983). *J. Am. Chem. Soc.* **105**, 1332–1339.

WILLIAMSON, M. P. & WILLIAMS, D. H. (1981). *J. Am. Chem. Soc.* **103**, 6580–6585.

WILSON, A. J. C. (1976). *Acta Cryst.* A**32**, 994–996.